Journal of Magnetic Resonance 194 (2008) 136–146

Contents lists available at ScienceDirect

Journal of Magnetic Resonance

journal homepage: www.elsevier.com/locate/jmr

A structure refinement strategy for NMR crystallography: An improved crystal structure of silica-ZSM-12 zeolite from ^{29}Si chemical shift tensors

Darren H. Brouwer *

Steacie Institute for Molecular Science, National Research Council of Canada, 100 Sussex Drive, Ottawa, Ont., Canada K1A 0R6

ARTICLE INFO

Article history:
Received 10 April 2008
Revised 26 June 2008
Available online 2 July 2008

Keywords:
Zeolites
NMR crystallography
Chemical shift anisotropy
Crystal structure
Ab initio calculations

ABSTRACT

A strategy for performing crystal structure refinements with NMR chemical shift tensors is described in detail and implemented for the zeolite silica-ZSM-12 (framework type code MTW). The ^{29}Si chemical shift tensors were determined from a slow magic-angle spinning spectrum obtained at an ultrahigh magnetic field of 21.1 T. The Si and O atomic coordinate parameters were optimized to give the best agreement between experimentally measured and *ab initio* calculated principal components of the ^{29}Si chemical shift tensors, with the closest Si–O, O–O, and Si–Si distances restrained to correspond with the distributions of the distances found in a set of single-crystal X-ray diffraction (XRD) structures of high-silica zeolites. An improved structure for the silica-ZSM-12 zeolite, compared to a prior structure derived from powder XRD data, is obtained in which the agreement between the experimental and calculated ^{29}Si chemical shift tensors is dramatically improved, the Si–O, O–O, and Si–Si distances correspond to the expected distributions, while the calculated powder XRD pattern remains in good agreement with the experimental powder XRD data. It is anticipated that this "NMR crystallography" structure refinement strategy will be an important tool for the accurate structure determination of materials that are difficult to fully characterize by traditional diffraction methods.

1. Introduction

Solid-state NMR spectroscopy is emerging as an important technique for structure determination of crystalline solids as researchers develop innovative ways to link advances in NMR pulse sequence design, *ab initio* methods for calculation of NMR parameters, magic-angle spinning (MAS) technology, and higher magnetic fields with modeling, quantum-chemical calculations, and the crystallography that is traditionally carried out with diffraction methods. The general philosophy behind "NMR crystallography" is to incorporate the wide variety of information available in solid-state NMR experiments into the process of crystal structure determination, typically in combination with other structural characterization methods and computational chemistry, and particularly for those materials for which it is difficult to obtain suitably large single crystals for diffraction experiments.

The areas of present research in NMR crystallography can be roughly categorized according to the classes of materials being studied: inorganic "network" materials such as zeolites and related materials [1–8], organic molecular crystals [9–17], and bio-molecules [18–23]. The challenges for each class of materials are somewhat different. For inorganic network materials such as zeolites, the challenge is to establish the "infinite" covalent and/or ionic structure that defines the crystal structure. For organic molecular crystals, the challenge is to define both the molecular conformation and molecular packing which are often determined by weak intermolecular interactions such as hydrogen bonding. It could be argued that the work in biomolecules is not true NMR crystallography in the sense that the objective is usually to establish the molecular conformations of the individual peptide or protein molecules (albeit often large and complicated molecules), whereas NMR crystallography generally refers to establishing the full crystal structure. Nonetheless, this work is very impressive and shares similar challenges and strategies to the other classes of materials.

The process of structure determination of crystalline solids generally involves three main stages. First, the long-range periodicity of the crystal structure, as defined by the lattice parameters and the space group, is established. Second, an initial structural model (or a set of structural models) is derived or *solved* from the available data. Lastly, the structural model is typically *refined* or optimized to give the best agreement with the available data. The term "solved" here does not refer to fully determining the structure, but rather to deriving a trial or model structure from the available experimental data—be it from diffraction, NMR, modeling, any other method, or a combination of methods—and allowing the process of structure determination to continue to the refinement stage. In practice, these three main steps may not be so

* Fax: +1 613 998 7833.
E-mail address: Darren.Brouwer@nrc-cnrc.gc.ca

1090-7807/$ - see front matter
doi:10.1016/j.jmr.2008.06.020

clearly distinguished from one another. For example, if a "solved" trial structure does not refine sufficiently well, it could be necessary to return to the first or second stages to find a different structure. Or, it is possible that several trial structures are derived in the structure solution stage and it is only by attempting to refine each of these structures that the correct structure emerges.

For each of these main stages, NMR researchers are finding creative ways to incorporate the information available from solid-state NMR experiments. For instance, the number of peaks observed in an NMR spectrum and their relative intensities can provide key information about the identity of the crystal's asymmetric unit and space group [24–26]. These concepts have recently been formalized [27] and NMR experiments to identify the local site symmetry have been presented [28]. Two-dimensional (2D) correlation experiments, in which proximities and connectivities between atoms can be established, may also be employed to identify possible space groups [29], to aid in assignment of the NMR resonances [13,30–39], or to derive structural models [7,8]. The distance information provided by solid-state NMR can be used to derive or constrain structural models [5,6,40–42] in combination with other methods. In some cases, 2D correlation experiments have even been extended to an additional dimension in order to provide short and long-range distance information that has been used to actually *solve* crystal structures directly from the NMR data alone [1,2] or in combination with molecular modeling [9,10].

The combination of measurements and quantum-chemical calculations of NMR parameters (such as chemical shifts, quadrupolar parameters, and even J-couplings) has also become an important and very sensitive tool for probing the local environments in crystal structures [3,4,11–17,37,38,43–53]. There have been tremendous recent advances in quantum-chemical calculation methods for periodic systems [54,55] that enable the calculation of NMR parameters for solid crystalline materials [11–13,37,38,44–46]. Chemical shift measurements and calculations have been combined to provide structural constraints such as dihedral angles [15,53] which can be useful information for direct-space search methods for solving structures from powder XRD data [15,16,56]. Due to the high sensitivity of these NMR parameters to small changes in local structure, it is possible to couple quantum-chemical calculations with experimental measurements in order to distinguish between proposed crystal structures [16,17,47] and verify refined structures [11,39,57,58]. Furthermore, it is now becoming possible to incorporate NMR parameters directly in crystal structure refinements [4,58]. It is the use of chemical shift tensors for NMR crystallography, particularly for the refinement of zeolite crystal structures that is the focus of this paper.

It has recently been shown that zeolite ^{29}Si chemical shift (CS) tensors can be accurately measured at an ultrahigh magnetic field (21.1 T) either by slow MAS or a 2D chemical shift anisotropy (CSA) recoupling experiment [3]. Since the ^{29}Si CS tensors tend to have small anisotropies due to the Si atoms being located in near-tetrahedral SiO_4 geometries in zeolite frameworks, performing the measurements at a high magnetic field strength is advantageous since the CSA (in hertz) scales with the field strength. Hartree–Fock *ab initio* calculations of the corresponding ^{29}Si shielding tensors, calculated on clusters extracted from the zeolite crystal structures, were found to be in excellent agreement with the experimental measurements. The quality of the agreement between experiments and calculations was strongly dependent on the quality of the crystal structure used for the quantum-chemical NMR calculations: crystal structures derived from single-crystal XRD gave calculated ^{29}Si CS tensors that were in far better agreement with experimental measurements than those determined from crystal structures derived from powder XRD data.

This strong sensitivity of the ^{29}Si CS tensors to the local structural environment of each Si atom forms the basis of the work described briefly in a recent communication [4] and in greater detail here in which the measurement and calculation of ^{29}Si chemical shift tensors are incorporated into an NMR crystallography *structure refinement* tool for zeolite crystal structure determination. The Si and O coordinates of the zeolite framework are optimized or "refined" to give the best agreement between experimentally measured and *ab initio* calculated principal components of the ^{29}Si CS tensors (with additional restraints on the closest Si–O, O–O, and Si–Si distances). This structure refinement tool complements the recently described method for *structure solution* of zeolite frameworks in which the Si coordinates are solved from ^{29}Si double quantum (DQ) NMR data [1,2] since these solved structures are not highly accurate and the oxygen atomic positions are not known.

It was demonstrated in a recent communication that the framework structure of the zeolite Sigma-2 could be solved from ^{29}Si DQ NMR data and subsequently refined against the ^{29}Si CS tensors to give a complete NMR-determined crystal structure of the zeolite framework that was in very good agreement with the single-crystal XRD structure [4]. The aim of this paper is to describe this particular structure refinement strategy in much greater detail and to apply it to the structure of zeolite silica-ZSM-12 (hereafter referred to as just ZSM-12) for which the existing crystal structure derived from powder XRD data [26] has been shown to give poor agreement between the calculated and experimental ^{29}Si CS tensors [3]. The structure of ZSM-12 is displayed in Fig. 1. The framework type code [59] for ZSM-12 is MTW.

A structure for ZSM-12 was originally proposed by LaPierre et al. based on electron diffraction, powder X-ray diffraction, and model building [60]. Fyfe et al. subsequently collected high resolution ^{29}Si MAS NMR spectra and high resolution synchrotron powder XRD data for ZSM-12 [26] and demonstrated that there exists a subtle pseudo-symmetry problem with the structure requiring a doubling of one of the unit cell parameters. The NMR data was important for identifying the correct space group. A structure refinement of the Si and O coordinates (without restraints) against the synchrotron powder XRD data was performed with a parameter to correct for preferred crystallite orientation effects.

There are some indications in this initial report of the ZSM-12 structure [26] that the refined crystal structure, although correct in the general sense, is not highly accurate. An analysis of the Si–O bond lengths, O–O distances, and Si–O–Si bond angles revealed broader ranges than expected. Furthermore, an attempt to assign the peaks in the ^{29}Si NMR spectrum to the crystallographic sites using empirical correlations between isotropic ^{29}Si chemical shifts

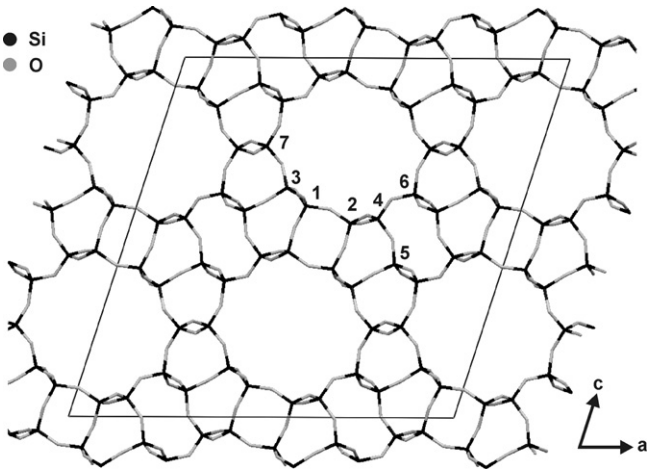

Fig. 1. NMR-refined crystal structure of silica-ZSM-12 (framework type code MTW) with Si sites labeled and unit cell indicated.

and mean Si–Si bond lengths [61] gave an assignment that contradicted the unambiguous assignment derived from 2D correlation experiments [30,31]. It was concluded that since minor changes in the local environment of the Si atoms lead to significant changes in the isotropic chemical shifts, and since the errors in powder diffraction are relatively large, one must be very careful in using geometrical data derived from powder XRD structures to correlate with isotropic chemical shift data [26]. This was bore out in a later paper in which the correlations between geometrical parameters and isotropic ^{29}Si chemical shifts were found to significantly improve after powder XRD derived zeolite crystal structures were subjected to lattice energy minimization calculations [62], although these calculations were not carried out for ZSM-12.

Finally, the recent paper [3] describing measurements and *ab initio* calculations of ^{29}Si CS tensors clearly indicated that the existing powder XRD crystal structure for ZSM-12 was not very accurate since the quality of agreement between experimental and calculated ^{29}Si CS tensor components was very poor, whereas the quality of agreement for other zeolites with crystal structures derived from higher quality single-crystal XRD data was very good. In this paper, an improved crystal structure for ZSM-12 is determined from solid-state NMR data that gives very good agreement with experimental and calculated ^{29}Si CS tensors, has Si–O, O–O, and Si–Si distances consistent with the expected distributions of these distances, and remains in good agreement with the powder XRD pattern.

2. Experimental

Solid-state NMR experiments were carried out on a Bruker AVANCE-II 900 MHz NMR spectrometer operating at a magnetic field of 21.1 T (178.831 MHz ^{29}Si Larmor frequency) using a standard-bore double resonance 4 mm MAS NMR probe. The ^{29}Si chemical shifts were referenced by setting the ^{29}Si resonance for a sample of neat liquid tetramethylsilane (TMS) sealed in a 3 mm glass tube to 0 ppm.

Spectrum fitting of the slow spinning MAS spectrum, in order to estimate the span Ω and skew κ values and their uncertainties, was carried out according to the following protocol. The spectra were first deconvoluted to give the amplitudes of the spinning sidebands for each isotropic peak. A series of spinning sideband patterns were calculated for $10 \leqslant \Omega \leqslant 35$ ppm in steps of 1 ppm and $-1 \leqslant \kappa \leqslant 1$ in steps of 0.1 and each of these was fit to the experimental amplitudes by adjusting a scaling parameter to minimize the sum of the squares of the differences, χ^2_{ssb}. Contour plots of χ^2_{ssb} as a function of Ω and κ were constructed to locate the values of Ω and κ giving the minimum χ^2_{ssb} and the uncertainties in Ω and κ were estimated from the values of Ω and κ giving χ^2_{ssb} values with twice the minimum value of χ^2_{ssb}. The principal components $\delta_{11} \geqslant \delta_{22} \geqslant \delta_{33}$ were calculated using the relations $\delta_{iso} = (\delta_{11} + \delta_{22} + \delta_{33})/3$, $\Omega = \delta_{11} - \delta_{33}$, and $\kappa = (3\delta_{22} - \delta_{iso})/\Omega$, while their uncertainties were determined from the widest possible ranges of their values given the uncertainties in δ_{iso}, Ω, and κ.

Ab initio Hartree–Fock calculations were performed with Gaussian98 (revision A.11.3) [63] using the gauge including atomic orbital (GIAO) method for NMR shielding calculations. The calculations were carried out on clusters extracted from the crystal structures with the Si site of interest at the core of each cluster. Each central Si atom was surrounded by at least three coordination spheres with the outer oxygen atoms terminated with hydrogen atoms placed 0.96 Å from the oxygen atom along the O–Si bond vector to the Si in the next coordination sphere (that is not included in the cluster). In the case of some clusters in which the atoms in the outer coordination spheres close in on one another to form 4-rings, an additional Si atom was included to close the ring along with two additional oxygen atoms and terminating H atoms. This is the same general strategy for extracting clusters from crystal structures employed in previous work [3,4,47,64,65]. The calculations employed 6-311G(2df) basis sets for the central Si atom, nearest neighbour O atoms, and next-nearest neighbour Si atoms while the outer O and H atoms employed 6-31G basis sets. To facilitate comparison of calculated and experimental chemical shifts, the calculated shielding tensor values were converted into chemical shift values using α-quartz as a secondary chemical shift standard. The calculated absolute shielding values, σ, were converted to relative chemical shifts, δ, with respect to TMS using:

$$\delta^{TMS}(\text{cluster}) = \sigma_{iso}(\alpha\text{-quartz}) + \delta^{TMS}_{iso}(\alpha\text{-quartz}) - \sigma(\text{cluster}) \quad (1)$$

where σ_{iso}(α-quartz) and σ(cluster) were calculated using the same basis sets and cluster size. The experimentally observed isotropic chemical shift for α-quartz was $\delta^{TMS}_{iso}(\alpha\text{-quartz}) = -107.28$ppm [3] and the calculated absolute isotropic shielding (using the coordinates from a single crystal XRD structure [66]) value was σ_{iso}(α-quartz) = 491.19 ppm. These conditions for cluster size and basis sets have been established in previous work [3,4] to give accurate calculation results.

The *ab initio* calculations of NMR parameters were carried out in parallel on a computer cluster with 100 nodes, 20 of which were available for these calculations. Powder XRD patterns were calculated using the online calculation tool available on the zeolite structure database website [59]. All other calculations and were carried out using a notebook written for *Mathematica* 6.0 [67].

3. Structure refinement

The goal of the structure refinement procedure was to find the set of Si and O atomic coordinates giving the best agreement between experimentally measured and *ab initio* calculated ^{29}Si CS tensor components, with restraints on the closest Si–O, O–O, and Si–Si distances. The function that was minimized is:

$$\chi^2 = \chi^2_{CS} + \chi^2_{dist} \quad (2)$$

The first term, χ^2_{CS}, is the quality of agreement between experimental, $\delta^{(s)\exp}_{ii}$, and *ab initio* calculated, $\delta^{(s)\text{calc}}_{ii}$, CS tensor components:

$$\chi^2_{CS} = \sum_{s=1}^{N_{Si}} \sum_{i=1}^{3} \left\{ \left(\delta^{(s)\,\exp}_{ii} - \delta^{(s)\text{calc}}_{ii} \right) / \sigma^{(s)}_{ii} \right\}^2 \quad (3)$$

where $s = 1 \ldots N_{Si}$ denotes the Si site, i denotes the principal component, and $\sigma^{(s)}_{ii}$ is the estimated uncertainty of the corresponding principal ^{29}Si CS tensor component. The second term, χ^2_{dist}, restrains the closest Si–O, O–O, and Si–Si distances to expected values:

$$\chi^2_{dist} = \sum_{\Lambda} \sum_{j} \left\{ \left(r^{(j)}_{\Lambda} - r^{*}_{\Lambda} \right) / \sigma_{\Lambda} \right\}^2 \quad \Lambda = \text{Si—O, O—O, Si—Si} \quad (4)$$

where $r^{(j)}_{\Lambda}$ represents the closest distances calculated from the model structure and r^{*}_{Λ} and σ_{Λ} are the target distances and standard deviations. The target Si–O, O–O, and Si–Si distances and standard deviations were 1.60 ± 0.01, 2.61 ± 0.02, and 3.10 ± 0.05 Å respectively. These values are consistent with the distributions of distances compiled from the following set of single-crystal XRD structures of high-silica zeolites: Sigma-2 [3], ZSM-5 [68], Ferrierite [69], ITQ-4 [70], and Theta-1 [71] (see bottom of Fig. 4).

The χ^2 value above can be alternatively expressed as

$$\chi^2(\mathbf{x}) = \sum_{i=1}^{m} r_i(\mathbf{x})^2 \quad (5)$$

with the following definitions: $\mathbf{x} = \{x_1, \ldots, x_n\}$ is the set of parameters being optimized (Si and O atomic coordinates); $\mathbf{y} = \{y_1, \ldots, y_m\}$ is the set of observations (experimental tensor components and target distances); $\mathbf{w} = \{w_1, \ldots, w_m\}$ is the set of corresponding weights

for each of the observations (inverses of the uncertainties of the tensor components and standard deviations of the target distances); $\mathbf{f}(\mathbf{x}) = \{f_1(\mathbf{x}), \ldots f_m(\mathbf{x})\}$ is the set of calculated values for a given set of parameters $\mathbf{x}$ (the set of *ab initio* calculated tensor components and calculated distances for a given set of Si and O atomic coordinates); $\mathbf{r}(\mathbf{x}) = \{r_1(\mathbf{x}), \ldots, r_m(\mathbf{x})\}$ where $r_i(\mathbf{x}) = w_i\{f_i(\mathbf{x}) - y_i\}$ is the set of weighted residuals for a given set of parameters $\mathbf{x}$ (the weighted differences between calculated tensor components and distances and the experimental tensor components and target distances).

In the ZSM-12 crystal structure there are 7 unique Si sites and 14 unique O sites. Since each site is on a general position (x, y, z) there were a total of $n = 21 \times 3 = 63$ parameters to be refined (the unit cell parameters were fixed to those determined by powder XRD [26]). There were $7 \times 3 = 21$ observed ^{29}Si CS tensor components and 28, 42 and 14 unique Si–O, O–O, and Si–Si distances, respectively, giving a total of $m = 105$ observations.

The minimization of χ^2 was carried out using the Gauss–Newton non-linear least-squares optimization algorithm as described in detail the book by Nocedal and Wright [72]. The implementation of this algorithm for the NMR structure refinement procedure is outlined here. The algorithm is an iterative process in which a new set of parameters $\mathbf{x}_{k+1}$ is derived from an existing set of parameters $\mathbf{x}_k$:

$$\mathbf{x}_{k+1} = \mathbf{x}_k + \Delta\mathbf{x}_k \tag{6}$$

by first determining a vector $\mathbf{p}$ that describes the direction in which to step and secondly determining a scalar value α that describes how far to step in this direction:

$$\Delta\mathbf{x}_k = \alpha\mathbf{p} \tag{7}$$

The step direction vector $\mathbf{p}$ is calculated from the Jacobian matrix $\mathbf{J}$ according to:

$$\mathbf{p} = (\mathbf{J}^T\mathbf{J})^{-1} \cdot \mathbf{J}^T \cdot \mathbf{r}(\mathbf{x}_k) \tag{8}$$

where $\mathbf{J}$ is an $m \times n$ matrix of partial derivatives of each weighted residual against each parameter. The elements of the Jacobian matrix are $J_{ij} = \partial r_i/\partial x_j$ and the full matrix is:

$$\mathbf{J} = \begin{pmatrix} \partial r_1/\partial x_1 & \cdots & \partial r_1/\partial x_n \\ \vdots & \ddots & \vdots \\ \partial r_m/\partial x_1 & \cdots & \partial r_m/\partial x_n \end{pmatrix} \tag{9}$$

These partial derivatives were numerically estimated by evaluating the change in the residuals with small changes in the values of the parameters:

$$J_{ij} = \frac{r_i(\mathbf{x} + \boldsymbol{\varepsilon}_j) - r_i(\mathbf{x})}{\varepsilon} \tag{10}$$

where $\boldsymbol{\varepsilon}_j$ is a vector of zeroes except for the jth element which is a very small amount ε such that

$$\mathbf{x} + \boldsymbol{\varepsilon}_j = \{x_1, \ldots, x_j + \varepsilon, \ldots, x_n\}. \tag{11}$$

In this implementation, ε was set to 1×10^{-5}.

Once the step direction vector $\mathbf{p}$ is determined, a *line search* is performed along this direction, in order to find the value of α that gives a *sufficient decrease* in χ^2 (see below). The implementation of the line search for this particular problem is described below while the full details of the line search algorithm can be found in ref [72].

The steps involved in the structure refinement procedure are outlined within the dashed-line box in Fig. 2. Starting from a structure parameter set $\mathbf{x}$, a series of new structure parameter sets $\mathbf{x} + \boldsymbol{\varepsilon}_j$ were constructed in which one of the structural parameters had been changed by a small amount ε. The crystal structures for each of these parameter sets were then constructed and the calculations of the Si–O, O–O, and Si–Si distances and the ^{29}Si CS tensor components were carried out for each crystal structure. The calculations

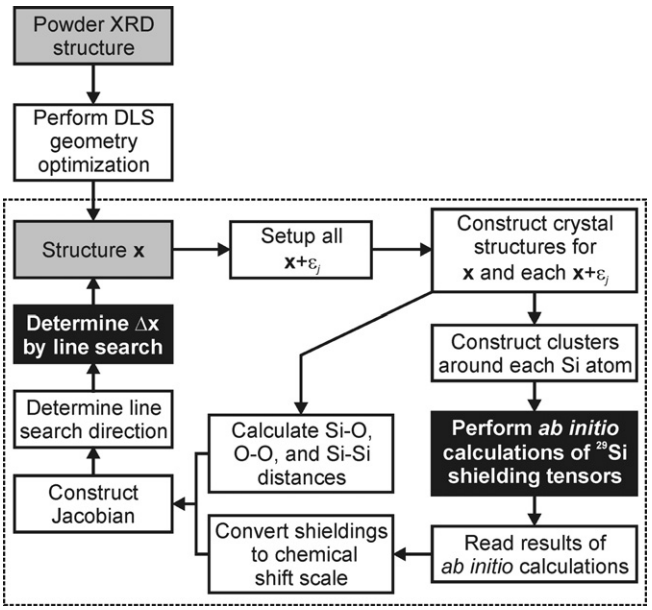

Fig. 2. Schematic diagram of the NMR structure refinement strategy. The black boxes denote steps in which *ab initio* calculations of ^{29}Si shielding tensors are carried out (see text for more details).

of the distances were relatively straightforward, but the ^{29}Si CS tensor component calculations required a series of steps.

The first step in the calculation of the ^{29}Si CS tensor components involved constructing a series of clusters around each unique Si site for each of the crystal structures. From these clusters, a subset of clusters was selected for *ab initio* NMR calculations: all of the clusters derived from structure $\mathbf{x}$ were chosen; however for the $\mathbf{x} + \boldsymbol{\varepsilon}_j$ structures, only those clusters were selected for which there was a small change in the position of the Si atom at the center of the cluster, one of the O atoms in the first coordination sphere, or one of the Si atoms in the second coordination sphere. It was assumed that a small change beyond the second coordination sphere had a negligible effect on the ^{29}Si CS tensor components calculated for the central Si atom and the corresponding partial derivative elements for the Jacobian matrix were assumed to be zero in these situations. For ZSM-12, the subset of clusters required to construct the Jacobian matrix consisted of 163 clusters. A series of Gaussian98 input files were constructed and the calculations were submitted to a computer cluster with 100 nodes, 20 of which were available for these calculations, allowing the cluster calculations to be performed in parallel. The calculation for each individual cluster took approximately 2–3 h and the calculations for all the clusters for a single iteration could be accomplished in less than a day. Once the *ab initio* calculations were finished, the Gaussian98 output files were read and the calculated ^{29}Si shielding tensor components were converted to the chemical shift scale according to Eq. (1).

The various results of the calculations of distances and CS tensor components were evaluated in order to construct the Jacobian matrix, which in turn was then used to calculate the line search direction according to Eq. (8). A series of new parameter sets were then constructed for the line search along this step direction and the distances and ^{29}Si CS tensor components were calculated in a similar fashion to the first stage (see below). Once a sufficient decrease in χ^2 was found, this new structure $\mathbf{x} + \Delta\mathbf{x}$ was passed on to the next iteration. The procedure is repeated until the χ^2 value did not improve significantly.

In the line search, a *sufficient decrease* in χ^2 is defined by the Wolfe conditions:

$$\chi^2(\mathbf{x}+\alpha\mathbf{p}) \leqslant \chi^2(\mathbf{x}) + c_1\alpha \mathrm{d}\chi^2(\mathbf{x}) \qquad (12)$$
$$|\mathrm{d}\chi^2(\mathbf{x}+\alpha\mathbf{p})| \leqslant -c_2\mathrm{d}\chi^2(\mathbf{x})$$

where c_1 and c_2 are constants (set to 0.0001 and 0.9, respectively, as suggested in ref [72]) and the $\mathrm{d}\chi^2$ terms denote the derivatives of the χ^2 function with respect to changes along the line search direction vector. These derivatives were estimated numerically according to:

$$\mathrm{d}\chi^2(\mathbf{x}) = \{\chi^2(\mathbf{x}+\varepsilon\mathbf{p}) - \chi^2(\mathbf{x})\}/\varepsilon \qquad (13)$$
$$\mathrm{d}\chi^2(\mathbf{x}+\alpha\mathbf{p}) = \{\chi^2(\mathbf{x}+\alpha\mathbf{p}+\varepsilon\mathbf{p}) - \chi^2(\mathbf{x}+\alpha\mathbf{p})\}/\varepsilon$$

To carry out the line search, a series of structural parameter sets ($\mathbf{x}$, $\mathbf{x}+\varepsilon\mathbf{p}$, $\mathbf{x}+\alpha\mathbf{p}$, and $\mathbf{x}+\alpha\mathbf{p}+\varepsilon\mathbf{p}$ with α initially set to 1 and ε set to 0.01) were first set up and the corresponding crystal structures were then constructed. The relevant Si–O, O–O, and Si–Si distances were calculated for each structure and *ab initio* calculations of the ^{29}Si CS tensor components for clusters around each Si site in each structure were carried out. For ZSM-12, this involved submitting 7 *ab initio* calculations for each of the structures, giving a total of 21 *ab initio* cluster calculations (since $\chi^2(\mathbf{x})$ was already known from the initial calculations for the Jacobian matrix). The results of these calculations were then combined to evaluate the various χ^2 and $\mathrm{d}\chi^2$ values and to check if the Wolfe conditions for a sufficient decrease in χ^2 were met for the new structure $\mathbf{x}+\alpha\mathbf{p}$. If the conditions were not met, a new value of α was calculated by cubic interpolation [72] using the information contained in $\chi^2(\mathbf{x})$, $\mathrm{d}\chi^2(\mathbf{x})$, $\chi^2(\mathbf{x}+\alpha\mathbf{p})$, and $\mathrm{d}\chi^2(\mathbf{x}+\alpha\mathbf{p})$. For the new value of α, a new set of structures were constructed and distance and *ab initio* calculations were carried out. This process was repeated until a value of α was found that satisfies the Wolfe conditions. For the refinement of ZSM-12, it was never necessary to consider more than one additional calculation for the line search, as $\alpha = 1$ usually satisfied the conditions and if it did not, the next interpolated value of α would satisfy the conditions.

Once χ^2 did not significantly improve and the optimization was deemed to have converged, the uncertainties in the parameters could be estimated from the square roots of the diagonal elements of the variance–covariance matrix $\mathbf{\Sigma}$ that is approximated by

$$\mathbf{\Sigma} \approx 1/2(\mathbf{J}^{\mathrm{T}}\mathbf{J})^{-1} \qquad (14)$$

where the Jacobian matrix $\mathbf{J}$ is calculated for the final set of optimized parameters $\mathbf{x}$.

In the previous communication [4], it was demonstrated that it was possible to perform a refinement of the Sigma-2 crystal structure against the ^{29}Si CS tensor components *alone*, without the Si–O, O–O, and Si–Si distance restraints. In this case, the atomic coordinate parameters were optimized to minimize χ^2_{CS} only (Eq. (3)). Since there were more parameters than observations, the problem was *under determined* ($m < n$) and an important modification needed to be made. Following the procedure described by Kelley [73], the Gauss–Newton algorithm could still be used, but the calculation of the line-search direction vector $\mathbf{p}$ derived from the Jacobian (calculated from partial derivatives of the CS tensor components alone) must be modified to:

$$\mathbf{p} = \mathbf{J}^{\dagger} \cdot \mathbf{r}(\mathbf{x}_k) \qquad (15)$$

where $\mathbf{J}^{\dagger}$ is the *pseudo-inverse* (also called the Moore–Penrose inverse) and is calculated using the singular-value decomposition method, as described in Ref. [73]. (This is actual a more general description of the Gauss–Newton algorithm since $\mathbf{J}^{\dagger} = (\mathbf{J}^{\mathrm{T}}\mathbf{J})^{-1}\cdot\mathbf{J}^{\mathrm{T}}$ when the problem is overdetermined with $m > n$). This situation is mentioned only for completeness sake since a refinement of the ZSM-12 crystal structure against the ^{29}Si CS tensor components without the distance restraints was not actually performed. It is important to mention that for Sigma-2, the refinements with and without distance restraints gave very similar structures that were both in very good agreement with the single-crystal XRD structure [4].

4. Results

^{29}Si MAS NMR spectra of ZSM-12 are presented in Fig. 3. At the higher MAS frequency (Fig. 3a), the seven crystallographically unique Si sites are clearly resolved. The high resolution of the spectrum is an indication of the high degree of structural order and crystallinity of the polycrystalline powder sample. These resonances have been previously assigned to the indicated Si sites with two-dimensional correlation experiments.[30,31] At the lower MAS frequency (Fig. 3b), the spinning sideband profiles remain resolved and it was possible to fit this spectrum (Fig. 3c) and extract the spinning sideband intensities for each Si sites (Fig. 3d). From these spinning sideband profiles, it was possible to estimate the ^{29}Si chemical shift tensor principal components. The experimental and best-fit spinning sideband intensities are compared in Fig. 3e for each site while Fig. 3f displays the corresponding χ^2_{ssb} contour plots from which the best-fit values for the span Ω and skew κ (and their uncertainties) were estimated. The determined ^{29}Si CS tensor components are listed in Table 1. The spans of the tensors range from about 15 to 30 ppm while the skews indicate that none of the tensors are axially symmetric.

The results of *ab initio* calculations of the ^{29}Si CS tensors carried out using the coordinates of the powder XRD structure of ZSM-12 [26] are presented in Fig. 4a. The agreement with the experimentally determined principal components is very poor: the χ^2_{CS} is 2313 while the root-mean-square (rms) deviation between the experimental and calculated tensor components is 7.6 ppm. Furthermore, the histogram plots of the Si–O, O–O, and Si–Si distances in this ZSM-12 structure (Fig. 4b–d) reveal that these distances do not correspond well the expected range of values (based on the distances observed in single crystal structures of zeolites): the χ^2_{dist} is 813 and the rms deviations from the expected distances are listed in the first column of Table 2. Together, the NMR and distance calculations suggest that the powder XRD structure of ZSM-12 is not very accurate and could be significantly improved.

As a first step towards improving the structure, a distance least-squares (DLS) geometry optimization [74] of the ZSM-12 structure was performed, starting from the coordinates of the powder XRD structure. In the DLS optimization, the Si and O atomic coordinates were adjusted to minimize χ^2_{dist}, the sum of the squares of the (weighted) differences between the Si–O, O–O, and Si–Si distances of the structure and corresponding target distances (see Eq. (4)). The Gauss–Newton optimization algorithm [72] was used to find the Si and O coordinates giving the minimum of χ^2_{dist}. This DLS-optimized structure has a dramatically improved χ^2_{dist} value of 20, with distances that are very close to the target distances (see Fig. 4f–h and the second column of Table 2). *Ab initio* calculations of the ^{29}Si CS tensor components were carried out for this DLS-optimized structure and Fig. 4e shows that the agreement with the experimental values is improved, however significant deviations remain (χ^2_{CS} =365 and the rms deviation is 2.9 ppm).

To further improve the structure, the full structure refinement protocol described above (^{29}Si CS tensors *and* distances) was carried out starting from the DLS-optimized coordinates. After five iterations of the Gauss–Newton optimization algorithm, the overall χ^2 converged to 81.2 with a dramatic improvement in χ^2_{CS} to 6.6 at the expense of an increase in χ^2_{dist} to 74.6. Fig. 4i presents the excellent agreement between the experimental and *ab initio* calculated ^{29}Si CS tensor components (rms of 0.3 ppm) while Fig. 4j–l and the third column of Table 2 indicate that the Si–O, O–O, and Si–Si distances are consistent with the distributions of distances found in the set of available single-crystal XRD structures [3,68–71] of high-silica zeolites (Fig. 4m–o).

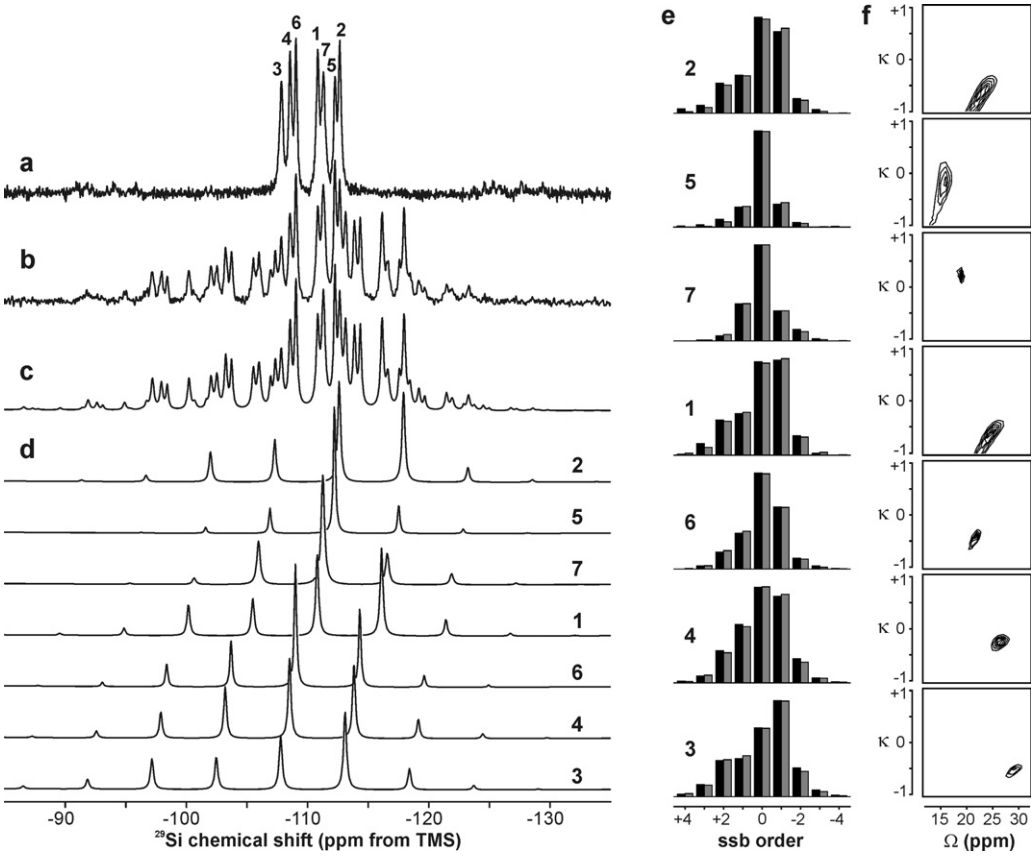

Fig. 3. (a and b) Experimental ^{29}Si MAS NMR spectra of ZSM-12 obtained at 21.1 T and MAS spinning frequencies of (a) 3000 Hz (128 scans) and (b) 950 Hz (512 scans) with recycle delays of 15 s. (c) Simulated 950 Hz MAS spectrum composed of (d) individual simulated spinning sideband patterns for each Si site. (e) Plots of spinning sideband intensities extracted from slow MAS spectrum (black) and calculated from best-fit values of Ω and κ (grey). (f) Contour plots of χ^2_{ssb} from which the best-fit values of Ω and κ and their uncertainties were estimated (see Table 1).

Table 1
Principal components of the ^{29}Si chemical shift tensors for ZSM-12[a]

Site	δ_{iso} (ppm)	Ω (ppm)	κ	δ_{11} (ppm)	δ_{22} (ppm)	δ_{33} (ppm)
Si2	−112.7 ± 0.1	22.8 ± 0.8	−0.65 ± 0.12	−98.8 ± 1.0	−117.6 ± 0.9	−121.6 ± 1.0
Si5	−112.3 ± 0.1	15.6 ± 0.7	−0.14 ± 0.16	−105.1 ± 0.9	−114.0 ± 0.9	−120.7 ± 0.9
Si7	−111.3 ± 0.1	18.8 ± 0.4	0.20 ± 0.07	−102.5 ± 0.5	−110.1 ± 0.6	−121.4 ± 0.5
Si1	−110.8 ± 0.1	25.0 ± 0.7	−0.61 ± 0.09	−95.8 ± 0.9	−115.9 ± 0.7	−120.8 ± 0.9
Si6	−109.1 ± 0.1	21.8 ± 0.4	−0.40 ± 0.06	−96.7 ± 0.6	−111.9 ± 0.5	−118.5 ± 0.6
Si4	−108.6 ± 0.1	26.1 ± 0.7	−0.27 ± 0.07	−94.3 ± 0.8	−110.9 ± 0.6	−120.4 ± 0.8
Si3	−107.8 ± 0.1	29.4 ± 0.6	−0.55 ± 0.05	−90.4 ± 0.7	−113.2 ± 0.5	−119.8 ± 0.7

[a] The isotropic shifts (δ_{iso}), span (Ω), and skew (κ) and their corresponding uncertainties were estimated from the spinning sideband profiles in Fig. 3 and then converted into the principal components $\delta_{11} \geqslant \delta_{22} \geqslant \delta_{33}$ using the relations $\delta_{iso} = (\delta_{11} + \delta_{22} + \delta_{33})/3$, $\Omega = \delta_{11} - \delta_{33}$, $\kappa = 3(\delta_{22} - \delta_{iso})/\Omega$.

The Si and O coordinates for this NMR-refined structure of ZSM-12 are listed in Table 3, along with the estimated uncertainties in the coordinates and the deviations of the atomic positions of the powder XRD structure [26] from this NMR-refined structure. The average estimated uncertainties for the Si and O atomic parameters of the NMR-refined structure are 0.035 and 0.060 Å, respectively (after conversion from fractional atomic coordinates). In almost every case, the deviations of the powder XRD atomic coordinates from the NMR-refined coordinates are significantly larger than the uncertainties. The average deviation (for all positions) is 0.124 Å while the average deviations for the Si and O positions are 0.080 and 0.145 Å respectively. While these values do seem small on their own, they are quite significant when compared to an expected Si–O bond length of 1.60 Å. On the other hand, it is striking how sensitive the ^{29}Si CS tensor components are to apparently small changes in the local environments: the improvement in the agreement by two orders of magnitude between the calculated and experimental ^{29}Si CS tensors from rms of 7.6 ppm for the powder XRD structure to 0.3 ppm for the NMR-refined structure (compare Fig. 4a to 4i) is achieved by changing the Si and O atomic positions by an average of only 0.124 Å.

Unfortunately, single crystals of ZSM-12 that would be suitably large enough for a single crystal XRD study are not presently available (this sample of ZSM-12 consists of crystallites with dimensions on the order of 1 μm), so it is not possible to comment directly on the accuracy of this NMR-refined structure. However, it has been demonstrated that the NMR-refined structure for Sigma-2 (using this same structure refinement strategy) was in very good agreement with a high quality single-crystal XRD structure with differences in the atomic coordinate parameters on the order of only 0.01 Å [4]. Hopefully, a single-crystal XRD structural study, either on a different sample with larger crystals and/or using a syn-

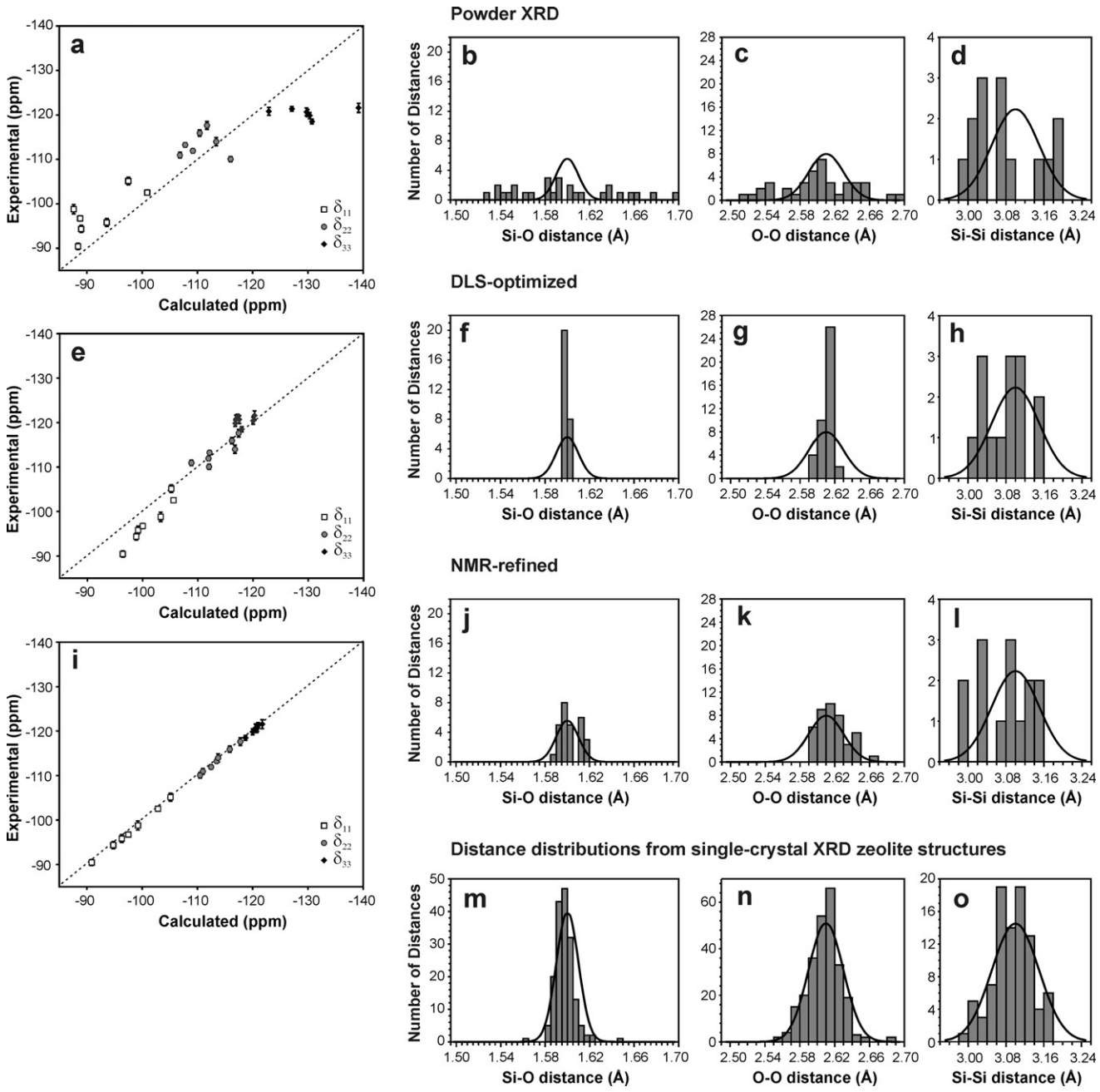

Fig. 4. (a, e and i) Quality of agreement between experimental and *ab initio* calculated principal components of ^{29}Si chemical shift tensors and (b, f and j) Si–O, (c, g and k) O–O, (d, h and l) Si–Si distance distribution histograms for structures of ZSM-12: (a–d) powder XRD structure [26], (e–h) structure after distance least-squares (DLS) geometry optimization, (i–l) structure after NMR refinement. The normal distributions (solid lines) correspond to the following target distances and standard deviations: 1.60 ± 0.01 Å, 2.61 ± 0.02 Å, and 3.10 ± 0.05 Å for Si–O, O–O, and Si–Si distances, respectively, which are consistent with the distributions of (m) Si–O, (n) O–O, and (o) Si–Si distances in a set of single-crystal XRD structures of high-silica zeolites [3,68–71].

Table 2
Various statistics for ZSM-12 structures describing quality of agreement between experimental and calculated ^{29}Si CS tensors as well as between actual and target distances

	Original PXRD	DLS-optimized	NMR refined
χ^2	3126	385	81.2
χ^2_{CS}	2313	365	6.6
χ^2_{dist}	813	20	74.6
rms(CS)	7.6 ppm	2.9 ppm	0.3 ppm
rms(Si–O)	0.045 Å	0.002 Å	0.009 Å
rms(O–O)	0.047 Å	0.007 Å	0.018 Å
rms(Si–Si)	0.068 Å	0.049 Å	0.057 Å

chrotron source, will be feasible at some point in the future to test the accuracy of the structure presented here.

The precision of the ZSM-12 structure is not as high as the Sigma-2 structure: the average uncertainties in the NMR-refined atomic coordinate parameters are 0.052 for ZSM-12 and 0.017 Å for Sigma-2, respectively. This is likely due to the slightly larger uncertainties in the ZSM-12 ^{29}Si CS tensor components (average uncertainties are 0.7 and 0.5 ppm for ZSM-12 and Sigma-2 respectively) and the lower ratio of observations and restraints to parameters of 1.67 for ZSM-12 compared to 2.3 for Sigma-2. The ratio of ^{29}Si CS tensor observations to parameters is 0.33 for ZSM-12 and is significantly lower than the ratio of 0.6 for Sigma-2.

Table 3
ZSM-12 fractional atomic coordinates[a] (and estimated uncertainties[b]) after refinement against ^{29}Si chemical shift tensors

Site	x	y	z	$\bar{\sigma}$ (Å)[c]	Δ (Å)[d]
Si1	0.0605(12)	0.016(8)	0.0868(7)	0.03	0.08
Si2	0.0689(12)	0.065(11)	0.9607(13)	0.04	0.05
Si3	0.3745(10)	0.014(8)	0.3628(09)	0.03	0.10
Si4	0.3644(12)	0.073(10)	0.5517(10)	0.03	0.05
Si5	0.2830(9)	0.080(14)	0.4273(9)	0.04	0.02
Si6	0.2893(10)	0.088(13)	0.1211(11)	0.04	0.11
Si7	0.2867(4)	0.037(18)	0.2469(6)	0.04	0.13
O1	0.0727(38)	−0.018(13)	0.0257(18)	0.07	0.12
O2	0.0042(12)	0.057(11)	0.9216(34)	0.06	0.15
O3	0.4255(15)	0.187(10)	0.8900(20)	0.04	0.08
O4	0.3306(22)	0.012(17)	0.8995(23)	0.06	0.10
O5	0.4068(28)	0.140(13)	0.0388(25)	0.06	0.28
O6	0.3419(18)	0.055(10)	0.7971(12)	0.04	0.19
O7	0.2587(42)	0.295(34)	0.2671(13)	0.10	0.32
O8	0.2406(21)	0.132(21)	0.5969(32)	0.08	0.11
O9	0.3455(16)	0.004(13)	0.1071(14)	0.04	0.06
O10	0.3088(18)	0.087(11)	0.4959(10)	0.04	0.23
O11	0.3020(18)	0.113(10)	0.1894(12)	0.04	0.12
O12	0.1019(22)	0.188(10)	0.6314(24)	0.05	0.13
O13	0.1064(19)	0.140(13)	0.4378(21)	0.05	0.04
O14	0.2319(19)	0.134(21)	0.9091(36)	0.08	0.10

[a] Space group: C2/c; cell parameters: a = 24.8633, b = 5.01238, c = 24.3275 Å, β = 107.7215°.
[b] The numbers in parentheses indicate the uncertainties in the last digit(s).
[c] $\bar{\sigma}$ =average of the uncertainties in the x, y, z parameters (in Å).
[d] Δ = deviation of atomic coordinates in original powder XRD structure from NMR-refined structure (in Å).

To compare the incredible sensitivity of NMR to local structure with powder XRD, the powder diffraction patterns for the starting and final structures were calculated and are compared in Fig. 5. The difference plot in Fig. 5c reveals only small differences between the two and these differences are certainly comparable to the residual between the experimental and calculated powder diffraction patterns presented in the previous work on the ZSM-12 structure (see Fig. 1 of Ref. [26]). The previous powder XRD work also reported complications arising from preferred orientation of the crystallites which may have led to errors in the resulting structure. Additionally, the bond distances and angles had not been restrained in the powder XRD refinement. The greatest deviations in the atomic coordinates of the powder XRD structure from the NMR-refined structure are observed for the O positions. This is not unsurprising since the O atoms are the weaker X-ray scatterers and the powder diffraction patterns are more sensitive to the Si atoms. In this NMR structure refinement approach, both Si *and* O coordinates are sensitive to the ^{29}Si CS tensors since both types of atoms play an important role in determining the magnetic shielding properties of the ^{29}Si nuclei.

5. Discussion

The structure refinement strategy presented here is significant advance in NMR crystallography, enabling the elucidation of crystal structures from solid-state NMR spectroscopy that are comparable to single-crystal XRD structures. The method is particularly powerful when combined with NMR methods for *solving* crystal structures [2]. Although these solution and refinement strategies have been applied to the determination of zeolite crystal structures, it is anticipated that these strategies could be adapted for application to other classes of materials. The aim of this section is to discuss some of the general features of this structure refinement strategy and how this work relates to the NMR crystallography strategies and tools being developed by others.

The structure refinement protocol described here requires significant computational resources. For the refinement of ZSM-12, each iteration required up to 200 *ab initio* cluster calculations: 163 to evaluate partial derivatives, construct the Jacobian matrix and determine the line search direction vector, and 21 or 35 additional calculations to determine the step length along this vector. However, this aim of this work was to demonstrate *proof of principle* that solid-state NMR and quantum-chemical calculations can indeed be used for refinement of crystal structures. There is certainly room for improvement in the computational efficiency of this strategy. Furthermore, computational resources are relatively cheap these days and are anticipated to become increasingly powerful. The structure refinement strategy is very easily parallelized and multi-node supercomputers are accessible to most computational chemists.

A potential criticism of this strategy is the inclusion of Si–O, O–O, and Si–Si distance restraints. It is worth making a comment about the distinction between *restraints* and *constraints* in the context of a structure refinement: a constraint is an exact condition which enables one or more variables to be expressed exactly in terms of other variables or constants and hence eliminated, whereas a restraint takes the form of additional information which is not exact but is subject to a realistic probability distribution [75]. The Si–O, O–O, and Si–Si distance restraints used here are consistent with

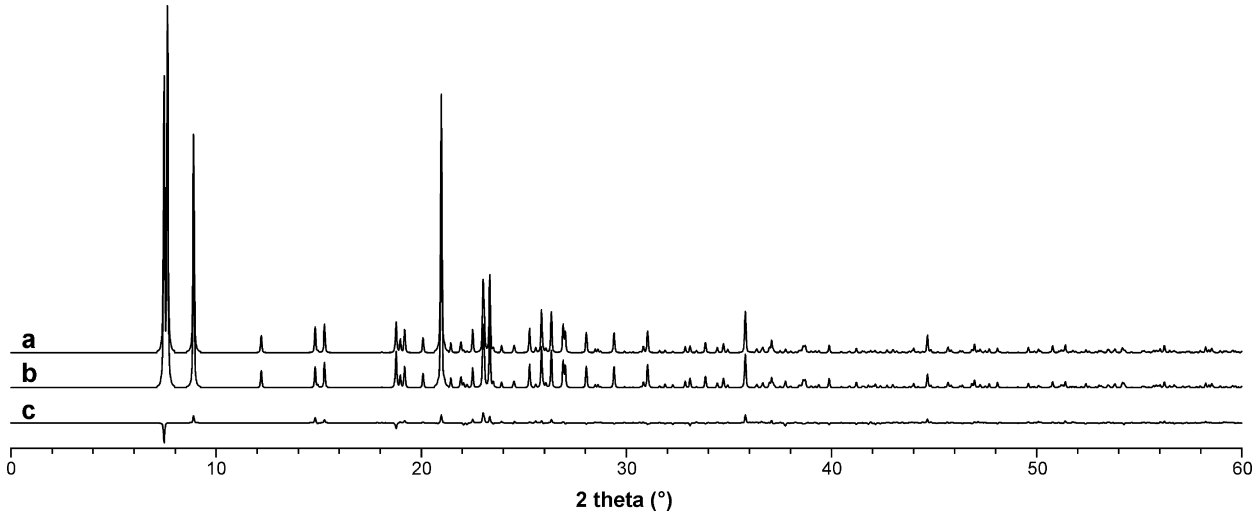

Fig. 5. Calculated powder XRD patterns for ZSM-12 structures: (a) powder XRD structure [26] and (b) NMR-refined structure; (c) difference between the two.

the distributions observed in a set of reliable single-crystal XRD zeolite crystal structures. Incorporating this information into the structure refinement is therefore a reasonable assumption and introduces valuable additional "observations". During the structure refinement, the distances are restrained to match these distributions, while yet retaining a degree of flexibility so that good agreement with the CS tensors components can be achieved. The inclusion of these distance restraints can be thought of performing a *combined* NMR and lattice-energy (to an approximation) minimization. Again, it is important to mention that for Sigma-2, the refinements with and without distance restraints gave very similar structures that were both in very good agreement with the single-crystal XRD structure [4]. For organic molecular solids and biomolecules, in which the molecular conformation is often sought, it is common practice to place constraints on most bond lengths and angles while certain bond angles or torsion angles are explored.

In the structure refinement presented here, the quantum-chemical calculations were carried out on *clusters* extracted from the crystal structure. This is clearly an approximation to the actual crystal structure. However, it has been demonstrated that ^{29}Si CS tensors in zeolites can be very accurately calculated with the appropriate cluster size and basis set [3]. The ^{29}Si shielding tensors seem to be primarily determined by the local structural geometry which can be adequately accounted for in clusters containing three coordination spheres around a central Si atom. However, it could potentially be more appropriate to carry out these calculations using the recent advances in quantum-chemical calculations of NMR parameters for periodic systems that are well-suited for calculations on crystal structures [46,54,55]. Certainly, there is no fundamental reason why the general structure refinement strategy outlined here could not be implemented using periodic density function theory (DFT) calculation methods such as CASTEP.

However, it should be pointed out that there are some advantages in performing traditional cluster calculations for zeolite ^{29}Si CS tensors. Zeolites tend to have unit cells with large volumes and many atoms. For example, the primitive unit cell for ZSM-12 has a volume of 1444 Å^3 and contains 84 atoms. Such a calculation with CASTEP is beyond the computing resources at our disposal (but certainly may not be for others). Furthermore, in order to numerically estimate the partial derivatives in the manner described here, an additional 63 of these large CASTEP calculations would have to be calculated at each iteration. On the other hand, by breaking down the crystal structure into clusters for Gaussian calculation, only 7 cluster calculations (of approximately 2–3 h each) are required to calculate all the ^{29}Si CS tensors and an additional 156 of these smaller cluster calculations are required to evaluate the partial derivatives. It is important to note that the validity of using cluster calculations for zeolite ^{29}Si CS tensors has been clearly established. For other systems such as organic molecular crystals or ionic solids, or for other NMR parameters such as quadrupolar interactions, it may not be possible to employ cluster calculations and periodic DFT calculations are likely to be essential. Perhaps there is room for improvement in how the partial derivatives of NMR parameters against atomic parameters are estimated.

To my knowledge, this structure refinement strategy presented here and in the recent communication [4] are the first examples of using quantum-chemical calculations of chemical shift tensors directly in a full crystal structure refinement procedure. However, there are notable recent examples of chemical shift information being used in the determination or validation of crystal structures. Witter et al. have reported a structure refinement of the I_α form of cellulose in which minimization of the differences between experimental and semi-empirical calculations of ^{13}C isotropic chemical shifts were combined with geometry optimization [58]. Semi-empirical calculations of the principal components of the ^{13}C tensor for the refined structure were compared to experimental ^{13}C tensors and used to validate the refined structure.

Grant and co-workers have combined the information from powder XRD, energy minimizations, and solid-state NMR measurements and quantum-chemical calculations of ^{13}C CS tensor components in an innovative way to solve the crystal structure of ambuic acid [16]. However, the refinement steps were either directly against the powder XRD data or were energy minimizations, rather than direct optimization against the CS tensor components. Harper and Grant have also described a procedure for using quantum-chemical calculations of ^{13}C CS tensors for evaluating computer-predicted crystal structures of organic molecular solids [17].

Chmelka and co-workers have proposed a structure for a surfactant-templated layered silicate material that was derived from 2D NMR data and subjected to lattice energy minimization [8]. Agreement between the experimental ^{29}Si isotropic chemical shifts and those calculated from the energy-minimized structure was used as additional evidence for the proposed structure. Similarly, Emsley and co-workers have used periodic DFT calculations of ^{1}H and ^{13}C isotropic chemical shifts to validate a periodic DFT energy-minimized crystal structure of an organic molecular solid [11] that was solved by combining molecular modeling and ^{1}H NMR spin diffusion data [10]. There are other examples of comparing quantum-chemical calculations of isotropic chemical shifts to experimental values for validation of crystal structures after energy minimization or powder XRD refinement [15,39,57].

In the area of biomolecules, one example of structure refinement using NMR data is the work on Gramacidin A monomer [22,23] in which dipolar and quadrupolar couplings and orientation of chemical shift tensors are used along with conformational energy terms to perfom a structure refinement, although the chemical shift tensors are not calculated using *ab initio* methods.

Another approach has been to use quantum-chemical calculations of chemical shifts (for example, as a function of dihedral angle) to establish the molecular conformation which is then used as a constraint or restraint in a direct space search algorithm for structure solution from powder XRD data [15,16]. Clearly, there are many ways in which experimental measurements and quantum-chemical calculations of chemical shifts can be incorporated into the determinations of crystal structures.

6. Conclusion

A structure of zeolite ZSM-12 has been determined by solid-state NMR and quantum-chemical calculations that gives a dramatic improvement over a previous powder XRD-derived structure [26] in the agreement between experimental and *ab initio* calculated ^{29}Si CS tensors while having Si–O, O–O, and Si–Si distances that are consistent with distance distributions derived from single-crystal structures. Furthermore, the structure remains consistent with the powder XRD data. This work demonstrates that solid-state NMR can be incredibly sensitive to the detailed local structure, to a far greater extent than powder XRD. This high sensitivity can be both helpful and a hindrance. Clearly, the high sensitivity allows for the structure refinement procedure described here and has been shown to give single-crystal quality structures from powders [4]. However, it is important to emphasize how crucial it is to have high quality structural information when quantum-chemical calculations of NMR parameters are carried out and compared to experimental data. As this example of ZSM-12 illustrates, errors on the order of 0.1–0.3 Å in the atomic coordinates can lead to extremely poor agreement between calculations and experiments (see Fig. 4a).

It is anticipated that the structure refinement strategy outlined in detail here could be extended to other classes of materials, incorporate experimental measurements and *ab initio* calculations

of other NMR parameters such as quadrupolar interaction parameters and *J*-couplings, and utilize the recent advances in *ab initio* DFT calculation methods for periodic systems. As solid-state NMR techniques, quantum-chemical calculations of NMR parameters, and their integration with diffraction methods continue to advance, NMR crystallography is expected to play an increasingly prominent role in the structural characterization of solids.

Acknowledgments

The ZSM-12 sample was provided by Colin Fyfe. Access to the 900 MHz NMR spectrometer was provided by the National Ultrahigh Field NMR Facility for Solids (Ottawa, Canada), a national research facility funded by the Canada Foundation for Innovation, the Ontario Innovation Trust, Recherche Québec, the National Research Council Canada, and Bruker BioSpin and managed by the University of Ottawa (www.nmr900.ca). The Natural Sciences and Engineering Research Council of Canada (NSERC) is acknowledged for a Major Resources Support grant. Access to parallel computing resources was provided by Serguei Patchkovskii and the NRC-SIMS Theory & Computation group.

References

[1] D.H. Brouwer, P.E. Kristiansen, C.A. Fyfe, M.H. Levitt, Symmetry-based ^{29}Si dipolar recoupling magic angle spinning NMR spectroscopy: a new method for investigating three-dimensional structures of zeolite frameworks, J. Am. Chem. Soc. 127 (2005) 542–543.
[2] D.H. Brouwer, R.J. Darton, R.E. Morris, M.H. Levitt, A solid-state NMR method for solution of zeolite crystal structures, J. Am. Chem. Soc. 127 (2005) 10365–10370.
[3] D.H. Brouwer, G.D. Enright, Probing local structure in zeolite frameworks: ultrahigh-field NMR measurements and accurate first-principles calculations of zeolite ^{29}Si magnetic shielding tensors, J. Am. Chem. Soc. 130 (2008) 3095–3105.
[4] D.H. Brouwer, NMR crystallography of zeolites: refinement of an NMR-solved crystal structure using *ab initio* calculations of ^{29}Si chemical shift tensors, J. Am. Chem. Soc. 130 (2008) 6306–6307.
[5] C.A. Fyfe, A.C. Diaz, H. Grondey, A.R. Lewis, H. Forster, Solid state NMR method for the determination of 3D zeolite framework/sorbate structures: ^{1}H/^{29}Si CP MAS NMR study of the high-loaded form of *p*-xylene in ZSM-5 and determination of the unknown structure of the low-loaded form, J. Am. Chem. Soc. 127 (2005) 7543–7558.
[6] C.A. Fyfe, D.H. Brouwer, Optimization, standardization, and testing of a new NMR method for the determination of zeolite host-organic guest crystal structures, J. Am. Chem. Soc. 128 (2006) 11860–11871.
[7] J. Dutour, N. Guillou, C. Huguenard, F. Taulelle, C. Mellot-Draznieks, G. Ferey, Chiolite, a case study for combining NMR crystallography, diffraction and structural simulation, Solid State Sci. 6 (2004) 1059–1067.
[8] N. Hedin, R. Graf, S.C. Christiansen, C. Gervais, R.C. Hayward, J. Eckert, B.F. Chmelka, Structure of a surfactant-templated silicate framework in the absence of 3D crystallinity, J. Am. Chem. Soc. 126 (2004) 9425–9432.
[9] B. Elena, L. Emsley, Powder crystallography by proton solid-state NMR spectroscopy, J. Am. Chem. Soc. 127 (2005) 9140–9146.
[10] B. Elena, G. Pintacuda, N. Mifsud, L. Emsley, Molecular structure determination in powders by NMR crystallography from proton spin diffusion, J. Am. Chem. Soc. 128 (2006) 9555–9560.
[11] C.J. Pickard, E. Salager, G. Pintacuda, B. Elena, L. Emsley, Resolving structures from powders by NMR crystallography using combined proton spin diffusion and plane wave DFT calculations, J. Am. Chem. Soc. 129 (2007) 8932–8933.
[12] R.K. Harris, P. Hodgkinson, C.J. Pickard, J.R. Yates, V. Zorin, Chemical shift computations on a crystallographic basis: some reflections and comments, Magn. Reson. Chem. 45 (2007) S174–S186.
[13] R.K. Harris, S. Cadars, L. Emsley, J.R. Yates, C.J. Pickard, R.K.R. Jetti, U.J. Griesser, NMR crystallography of oxybuprocaine hydrochloride, Modification II°, Phys. Chem. Chem. Phys. 9 (2007) 360–368.
[14] R.K. Harris, NMR crystallography: the use of chemical shifts, Solid State Sci. 6 (2004) 1025–1037.
[15] R.K. Harris, P. Ghi, R.B.Y. Hammond, C.Y. Ma, K.J. Roberts, J.R. Yates, C.J. Pickard, Solid-state NMR and computational studies of 4-methyl-2-nitroacetanilide, Magn. Reson. Chem. 44 (2006) 325–333.
[16] J.K. Harper, D.M. Grant, Y. Zhang, P.L. Lee, R. Von Dreele, Characterizing challenging microcrystalline solids with solid-state NMR shift tensor and synchrotron X-ray powder diffraction data: structural analysis of ambuic acid, J. Am. Chem. Soc. 128 (2006) 1547–1552.
[17] J.K. Harper, D.M. Grant, Enhancing crystal-structure prediction with NMR tensor data, Cryst. Growth Des. 6 (2006) 2315–2321.
[18] C.M. Rienstra, L. Tucker-Kellogg, C.P. Jaroniec, M. Hohwy, B. Reif, M.T. McMahon, B. Tidor, T. Lozano-Perez, R.G. Griffin, *De novo* determination of peptide structure with solid-state magic-angle spinning NMR spectroscopy, Proc. Natl. Acad. Sci. 99 (2002) 10260–10265.
[19] F. Castellani, B. van Rossum, A. Diehl, M. Schubert, K. Rehbien, H. Oschkinat, Structure of a protein determined by solid-state magic-angle spinning NMR spectroscopy, Nature 420 (2002) 98–102.
[20] C.P. Jaroniec, C.E. MacPhee, V.S. Bajaj, M.T. McMahon, C.M. Dobson, R.G. Griffin, High-resolution molecular structure of a peptide in an amyloid fibril determined by magic angle spinning NMR spectroscopy, Proc. Natl. Acad. Sci. 101 (2004) 711–716.
[21] S.G. Zech, A.J. Wand, A.E. McDermott, Protein structure determination by high-resolution solid-state NMR spectroscopy: Application to microcrystalline ubiquitin, J. Am. Chem. Soc. 127 (2005) 8618–8626.
[22] R. Bertram, J.R. Quine, M.S. Chapman, T.A. Cross, Atomic refinement using orientational restraints from solid-state NMR, J. Magn. Reson. 147 (2000) 9–16.
[23] R. Bertram, T. Asbury, F. Fabiola, J.R. Quine, T.A. Cross, M.S. Chapman, Atomic refinement with correlated solid-state NMR restraints, J. Magn. Reson. 163 (2003) 300–309.
[24] G.E. Balimann, G.J. Groombridge, R.K. Harris, K.J. Paker, B.J. Say, S.F. Tanner, Chemical applications of high-resolution ^{13}C NMR spectra for solids, Phil. Trans. R. Soc. Lond. Ser. A 299 (1981) 643–663.
[25] E. Gaudin, F. Boucher, M. Evain, F. Taulelle, NMR selection of space groups in structural analysis of Ag_7PSe_6, Chem. Mater. 12 (2000) 1715–1720.
[26] C.A. Fyfe, H. Gies, G.T. Kokotailo, B. Marler, D.E. Cox, Crystal structure of silica-ZSM-12 by the combined use of high-resolution solid state NMR spectroscopy and synchrotron X-ray powder diffraction, J. Phys. Chem. 94 (1990) 3718–3721.
[27] F. Taulelle, NMR crystallography: crystallochemical formula and space group selection, Solid State Sci. 6 (2004) 1053–1057.
[28] J. Senker, L. Seyfarth, J. Voll, Determination of rotational symmetry elements in NMR crystallography, Solid State Sci. 6 (2004) 1039–1052.
[29] I.J. King, F. Fayon, D. Massiot, R.K. Harris, J.S.O. Evans, A space group assignment of ZrP_2O_7 obtained by solid state ^{13}P NMR, Chem. Commun. (2001) 1766–1767.
[30] C.A. Fyfe, Y. Feng, H. Gies, H. Grondey, G.T. Kokotailo, Natural-abundance two-dimensional solid-state silicon-29 NMR investigations of three-dimensional lattice connectivities in zeolite structures, J. Am. Chem. Soc. 112 (1990) 3264–3270.
[31] C.A. Fyfe, H. Gies, Y. Feng, G.T. Kokotailo, Determination of three-dimensional lattice connectivities in zeolites using natural-abundance ^{29}Si two-dimensional NMR and the direct observation of ^{29}Si–O–^{29}Si couplings, Nature 341 (1989) 223–225.
[32] D.H. Brouwer, An efficient peak assignment algorithm for two-dimensional NMR correlation spectra of framework structures, J. Magn. Reson. 164 (2003) 10–18.
[33] C.A. Fyfe, H.M. zu Altenschildesche, K.C. Wong-Moon, H. Grondey, J.M. Chezeau, 1D and 2D solid state NMR investigations of the framework structure of as-synthesized $AlPO_4$-14, Solid State Nucl. Magn. Reson. 9 (1997) 97–106.
[34] W.A. Dollase, M. Feike, H. Forster, T. Schaller, I. Schnell, A. Sebald, S. Steuernagel, A 2D ^{13}P MAS NMR study of polycrystalline $Cd_3(PO_4)_2$, J. Am. Chem. Soc. 119 (1997) 3807–3810.
[35] V. Munch, F. Taulelle, T. Loiseau, G. Férey, A.K. Cheetham, S. Weigel, G.D. Stucky, A set of two-dimensional solid-state NMR experiments providing topological information for structure refinement of TMP-GaPO, Magn. Reson. Chem. 37 (1999) S100–S107.
[36] A. Lesage, C. Auger, S. Caldarelli, L. Emsley, Determination of through-bond carbon–carbon connectivities in solid-state NMR using the INADEQUATE experiment, J. Am. Chem. Soc. 119 (1997) 7867–7868.
[37] N. Mifsud, B. Elena, C.J. Pickard, A. Lesage, L. Emsley, Assigning powders to crystal structures by high-resolution ^{1}H-^{1}H double quantum and ^{1}H–^{13}C J-INEPT solid-state NMR spectroscopy and first principles computation. A case study of penicillin G, Phys. Chem. Chem. Phys. 8 (2006) 3418–3422.
[38] R.K. Harris, S.A. Joyce, C.J. Pickard, S. Cadars, L. Emsley, Assigning carbon-13 NMR spectra to crystal structures by the INADEQUATE pulse sequence and first principles computation: a case study of two forms of testosterone, Phys. Chem. Chem. Phys. 8 (2006) 137–143.
[39] R.A. Olsen, J. Struppe, D.W. Elliott, R.J. Thomas, L.J. Mueller, Through-bond ^{13}C–^{13}C correlation at the natural abundance level: refining dynamic regions in the crystal structure of vitamin-D_3 with solid-state NMR, J. Am. Chem. Soc. 125 (2003) 11784–11785.
[40] C.A. Fyfe, D.H. Brouwer, A.R. Lewis, J.M. Chezeau, Location of the fluoride ion in tetrapropylammonium fluoride silicalite-1 determined by ^{1}H/^{19}F/^{29}Si triple resonance CP, REDOR, and TEDOR NMR experiments, J. Am. Chem. Soc. 123 (2001) 6882–6891.
[41] C.A. Fyfe, D.H. Brouwer, A.R. Lewis, L.A. Villaescusa, R.E. Morris, Combined solid-state NMR and X-ray diffraction investigation of the local structure of the five-coordinate silicon in fluoride-containing as-synthesized STF zeolite, J. Am. Chem. Soc. 124 (2002) 7770–7778.
[42] D.A. Middleton, X. Peng, D. Saunders, K. Shankland, W.I.F. David, A.J. Markvardsen, Conformational analysis by solid-state NMR and its application to restrained structure determination from powder diffraction data, Chem. Commun. (2002) 1976–1977.
[43] R.K. Harris, P.Y. Ghi, R.B. Hammond, C.-Y. Ma, K.J. Roberts, Refinement of hydrogen atomic position in a hydrogen bond using a combination of solid-state NMR and computation, Chem. Commun. (2003) 2834–2835.

[44] J.R. Yates, T.N. Pham, C.J. Pickard, F. Mauri, A.M. Amado, A.M. Gil, S.P. Brown, An investigation of weak CH–O hydrogen bonds in maltose anomers by a combination of calculation and experimental solid-state NMR spectroscopy, J. Am. Chem. Soc. 127 (2005) 10216–10220.
[45] J.R. Yates, S.E. Dobbins, C.J. Pickard, F. Mauri, P.Y. Ghi, R.K. Harris, A combined first principles computational and solid-state NMR study of a molecular crystal: flurbiprofen, Phys. Chem. Chem. Phys. 7 (2005) 1402–1407.
[46] M. Profeta, F. Mauri, C.J. Pickard, Accurate first principles prediction of ^{17}O NMR parameters in SiO_2: assignment of the zeolite ferrierite spectrum, J. Am. Chem. Soc. 125 (2003) 541–548.
[47] L.M. Bull, B. Bussemer, T. Anupold, A. Reinhold, A. Samoson, J. Sauer, A.K. Cheetham, R. Dupree, A high-resolution ^{17}O and ^{29}Si NMR study of zeolite siliceous ferrierite and *ab initio* calculations of NMR parameters, J. Am. Chem. Soc. 122 (2000) 4948–4958.
[48] J.C. Facelli, D.M. Grant, Determination of molecular symmetry in crystalline naphthalene using solid-state NMR, Nature 365 (1993) 325–327.
[49] D.H. Barich, R.J. Pugmire, D.M. Grant, R.J. Iuliucci, Investigation of the structural conformation of biphenyl by solid-state ^{13}C NMR and quantum chemical NMR shift calculations, J. Phys. Chem. A 105 (2001) 6780–6784.
[50] J.K. Harper, J.C. Facelli, D.H. Barich, G. McGeorge, A.E. Mulgrew, D.M. Grant, 13C NMR investigation of solid-state polymorphism in 10-ceacetyl baccatin III, J. Am. Chem. Soc. 124 (2002) 10589–10595.
[51] M. Strohmeier, D.M. Grant, Experimental and theoretical investigation of the ^{13}C and ^{15}N chemical shift tensors in melanostatin-exploring the chemical shift tensor as a structural probe, J. Am. Chem. Soc. 126 (2004) 966–977.
[52] D.L. Bryce, G.D. Sward, S. Adiga, Solid-state $^{35/37}Cl$ NMR spectroscopy of hydrochloride salts of amino acids implicated in chloride ion transport channel selectivity: opportunities at 900 MHz, J. Am. Chem. Soc. 128 (2006) 2121–2134.
[53] S. Wi, H. Sun, E. Oldfield, M. Hong, Solid-state NMR and quantum chemical investigations of $^{13}C^{\alpha}$ shielding tensor magnitudes and orientations in peptides: determining ϕ and ψ torsion angles, J. Am. Chem. Soc. 127 (2005) 6451–6458.
[54] C.J. Pickard, F. Mauri, All-electron magnetic response with pseudopotentials: NMR chemical shifts, Phys. Rev. B 63 (2001) 245101.
[55] S.J. Clark, M.D. Segall, C.J. Pickard, P.J. Hasnip, M.I.J. Probert, K. Refson, M.C. Payne, First principles methods using CASTEP, Z. Kristallogr. 220 (2005) 567–570.
[56] R.B. Hammond, C. Ma, K.J. Roberts, P.Y. Ghi, R.K. Harris, Application of systematic search methods to studies of the structures of urea-dihydroxy benzene cocrystals, J. Phys. Chem. B 107 (2003) 11820–11826.
[57] M. Rajeswaran, T.N. Blanton, N. Zumbulyadis, D.J. Giesen, C. Conesa-Moratilla, S.T. Misture, P.W. Stephens, A. Huq, Three-dimensional structure determination of *N*-(*p*-tolyl)-dodecylsulfonamide from powder diffraction data and validation of structure using solid-state NMR spectroscopy, J. Am. Chem. Soc. 124 (2002) 14450–14459.
[58] R. Witter, U. Sternberg, S. Hesse, T. Kondo, F.T. Koch, A.S. Ulrich, ^{13}C chemical shift constrained crystal structure refinement of cellulose I_{α} and its verification by NMR anisotropy experiments, Macromolecules 39 (2006) 6125–6132.
[59] C. Baerlocher, L.B. McCusker, Database of zeolite structures: http://www.iza-structure.org/databases, 2007.
[60] R.B. LaPierre, A.C. Rohrman, J.L. Schlenker, J.D. Wood, M.K. Rubin, W.J. Rohrbaugh, The framework topology of ZSM-12: a high-silica zeolite, Zeolites 5 (1985) 346–348.
[61] C.A. Fyfe, Y. Feng, H. Grondey, Evaluation of chemical shift-structure correlations from a combination of X-ray diffraction and 2D MAS NMR data for highly siliceous zeolite frameworks, Micropor. Mater. 1 (1993) 393–400.
[62] M. Hochgrafe, H. Gies, C.A. Fyfe, Y. Feng, H. Grondey, Lattice energy-minimization calculation in the further investigation of XRD and NMR studies of zeolite frameworks, Chem. Mater. 12 (2000) 336–342.
[63] M.J. Frisch, G.W. Trucks, H.B. Schlegel, G.E. Scuseria, M.A. Robb, J.R. Cheeseman, V.G. Zakrzewski, J.A. Montgomery, Jr., R.E. Stratmann, J.C. Burant, S. Dapprich, J.M. Millam, A.D. Daniels, K.N. Kudin, M.C. Strain, O. Farkas, J. Tomasi, V. Barone, M. Cossi, R. Cammi, B. Mennucci, C. Pomelli, C. Adamo, S. Clifford, J. Ochterski, G.A. Petersson, P.Y. Ayala, Q. Cui, K. Morokuma, N. Rega, P. Salvador, J.J. Dannenberg, D.K. Malick, A.D. Rabuck, K. Raghavachari, J.B. Foresman, J. Cioslowski, J.V. Ortiz, A.G. Baboul, B.B. Stefanov, G. Liu, A. Liashenko, P. Piskorz, I. Komaromi, R. Gomperts, R.L. Martin, D.J. Fox, T. Keith, M.A. Al-Laham, C.Y. Peng, A. Nanayakkara, M. Challacombe, P.M.W. Gill, B. Johnson, W. Chen, M.W. Wong, J.L. Andres, C. Gonzalez, M. Head-Gordon, E.S. Replogle, J.A. Pople, Gaussian 98, Revision A.11.3, Gaussian, Inc., Pittsburgh PA, 2002.
[64] B. Bussemer, K.-P. Schroder, J. Sauer, Ab initio predictions of zeolite structures and ^{29}Si NMR chemical shifts, Solid State Nucl. Magn. Reson. 9 (1997) 155–164.
[65] X. Xue, M. Kanzaki, An ab initio calculation of ^{17}O and ^{29}Si NMR parameters for SiO_2 polymorphs, Solid State Nucl. Magn. Reson. 16 (2000) 245–259.
[66] L. Levian, C.T. Prewitt, D.J. Weidner, Structure and elastic properties of quartz at pressure, Am. Mineral. 65 (1980) 920–930.
[67] S. Wolfram, *Mathematica*: a system for doing mathematics by computer, version 6.0, Wolfram Media, Champaign, IL, 2007.
[68] H. van Koningsveld, J.C. Jansen, H. van Bekkum, The monoclinic framework structure of zeolite H-ZSM-5. Comparison with the orthorhombic framework of as-synthesized ZSM-5, Zeolites 10 (1990) 235–242.
[69] J.E. Lewis, C.C. Freyhardt, M.E. Davis, Location of pyridine guest molecules in an electroneutral $\{^{3\infty}\}[SiO_{4/2}]$ host framework: single-crystal structures of the as-synthesized and calcined forms of high-silica ferrierite, J. Phys. Chem. 100 (1996) 5039–5049.
[70] L.A. Villaescusa, P. Lightfoot, S.J. Teat, R.E. Morris, Variable-temperature microcrystal X-ray diffraction studies of negative thermal expansion in the pure silica zeolite IFR, J. Am. Chem. Soc. 123 (2001) 5453–5459.
[71] M.Z. Papiz, S.J. Andrews, A.M. Damas, M.M. Harding, R.M. Highcock, Structure of the zeolite Theta-1. Redetermination using single-crystal synchrotron-radiation data, Acta Cryst. C 46 (1990) 172–173.
[72] J. Nocedal, S.J. Wright, Numerical optimization, 1st ed., Springer, New York, 1999.
[73] C.T. Kelley, Iterative Methods for Optimization, Society for Industrial and Applied Mathematics, 1999.
[74] C. Baerlocher, A. Hepp., W.M. Meier, DLS-76: a program for the simulation of crystal structures by geometry refinement, Lab. f. Kristollographie, ETH, Zürich, 1978.
[75] P. Müller, R. Herbst-Irmer, A.L. Spek, T.R. Schneider, M.R. Sawaya, Crystal structure refinement: a crystallographer's guide to SHELXL, Oxford University Press, 2006.